

## DYNAMIC MECHANICAL PROPERTIES OF CARBON NANOTUBE- PEEK NANOCOMPOSITE

**D. Kaka<sup>\*</sup>, J. Rongong, A. Hodzic, C. Lord**

*Department of Mechanical Engineering, The University of Sheffield, Sheffield, S1 3JD, UK*

<sup>\*</sup>D. Kaka ([d.o.kaka@sheffield.ac.uk](mailto:d.o.kaka@sheffield.ac.uk))

**Keywords:** nanocomposite, carbon nanotube, PEEK, RVE.

### **Abstract**

*This research investigates the way in which the addition of carbon nanotubes modifies the dynamic mechanical properties of a high-performance thermoplastic polymer. In particular, the effects on stiffness and damping of the nanocomposite material over a range of temperatures and loading conditions were considered both experimentally and by numerical methods.*

*Tensile tests showed that the presence of nanotubes increased the stiffness and reduced the ductility. This resulted in an increase in strength at high temperature and a reduction at low temperature. Sinusoidal loading also showed that the modulus decreased and the damping increased as the excitation amplitude was increased.*

*Finite element analyses were carried out using representative volume element (RVE) for unidirectional distribution of nanotubes. The interface was modelled allowing bond slip between nanotube and polymer. Hyperelastic/viscoelastic effects were included using the experimentally measured material properties. The stiffness and loss factor were investigated under different conditions of bonding and fibre angle.*

### **1. Introduction**

Research into carbon nanotubes (CNTs) has been developed within different disciplines of science. Strong bonds between carbon atoms and their geometrical arrangements give nanotubes high strength, stiffness and thermal conductivity along with low density and electrical resistance. A polymer nanocomposite aims to utilise these properties by reinforcing a polymer matrix with fibre-like carbon nanotubes (with diameters of only a few nanometres). Key challenges that need to be overcome are to disentangle and disperse the nanotubes (as they tend to agglomerate) and to maximise the adhesion between the matrix and the nanotubes [1, 2]. Industrially applied processes are now being developed that can manufacture suitable nanocomposites [3].

Poly ether ether ketone (PEEK) is a high melting point, semi crystalline thermoplastic polymer that has high thermal and chemical stability, high elastic modulus and high strength (static, impact and fatigue) [4]. PEEK stiffness was improved by reinforcement of carbon-based fibres including CNTs. Some studies have reported increases in strength [3, 5] while others reported moderate increases in strength coupled with reductions in toughness, ductility and damping capacity [6, 7].

It is known that the nature of the interface zone between CNTs and the matrix is critical to the performance of a nanocomposite. The mechanical behaviour depends on the transfer of load from the matrix to the fibre, which relies on mechanical interlocking, chemical bonding, and van der Waals forces between the fibre and the matrix. Interfacial slippage and weak load transfer can cause reduced stiffness and strength [8, 9]. Functionalization of the CNTs is thought to increase the contact and hence adhesion between the fibre and the matrix. For example, functionalization with poly-sulfones was shown to increase toughness and stiffness of a CNT/PEEK composite [5].

Slip at the interface between the matrix and the nanotube has been identified as one mechanism for changes in damping seen experimentally [10, 11]. It has been shown that weak bonding can increase the interface slip and therefore increase the damping coefficient [12]. This effect has also been investigated numerically using representative volume element (RVE) methods [13]. Here, the nonlinear friction-type bond-slip between the fibre and the matrix was modelled by assuming different values of interfacial shear strength.

This study considers the behaviour of a nanocomposite made from functionalised CNTs and a thermoplastic polymer (PEEK). Dynamic mechanical properties were studied experimentally and theoretically over a range of temperatures and strain amplitudes.

## **2. Test specimens**

### *2.1 Materials and processing*

Test specimens were prepared from granulated PEEK (Victrex type 150p). These were first dried for 120 minutes at 150°C. Melting was carried out at 400°C and pressure of 550 bar. The material was then injected into a heated mould (200°C) and then allowed to cool to ambient temperature. The solidified specimens were of dog-bone shape with a gauge length of 28 mm, width of 4 mm and thickness of 2 mm.

The nanocomposite was produced by addition of 0.5 wt% functionalised nanotubes to PEEK. This was carried out by IMMAG according to the process described by Michelis and Vlachopoulos [3] with one difference: the final stage involving film stretching to realign nanotubes was not carried out. Instead, test specimens were prepared using the injection moulding as described above.

### *2.2 Transmission Electron Microscopy (TEM)*

The nanocomposite specimen was placed into epoxy (DDSA plus CY212 and BDMA) moulds and cured at 60°C for two days. Sections were produced using a Reichart Ultramicrotome with a diamond knife at 85 nm. These were collected onto coated copper grids and viewed in an FEI Tecnai 120 Biotwin TEM at an accelerating voltage of 80Kv. Images were recorded using a Gatan 600 CW digital camera.

TEM images in Figure 1 show the dispersion of nanotubes in PEEK. From TEM images, it can be observed that the nanotubes were well-separated, not strongly aligned and tended to agglomerate in some areas.

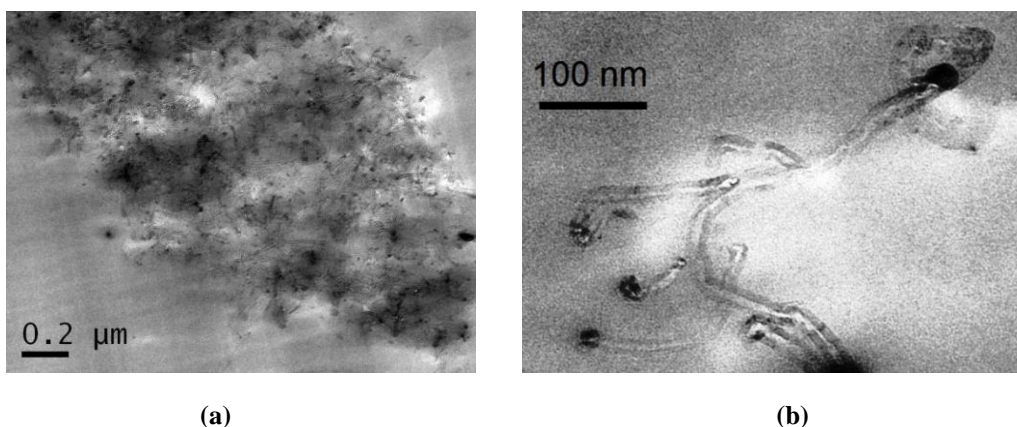


**Figure 1.** TEM images of functionalised CNT-PEEK, showing (a) CNT-PEEK interface and (b) non-aligned dispersion of CNTs .

### 3. Tensile test

The dog-bone shaped specimens were tested to failure in uniaxial tension using a MTS 858 Table Top hydraulic test machine. The tests were carried out at different temperatures and loading rates: at 25°C and 125°C the specimens were tested under speed rate of 0.1mm/min while at 160°C they were tested at a rate of 0.2mm/min. Results are presented in Figure 2.

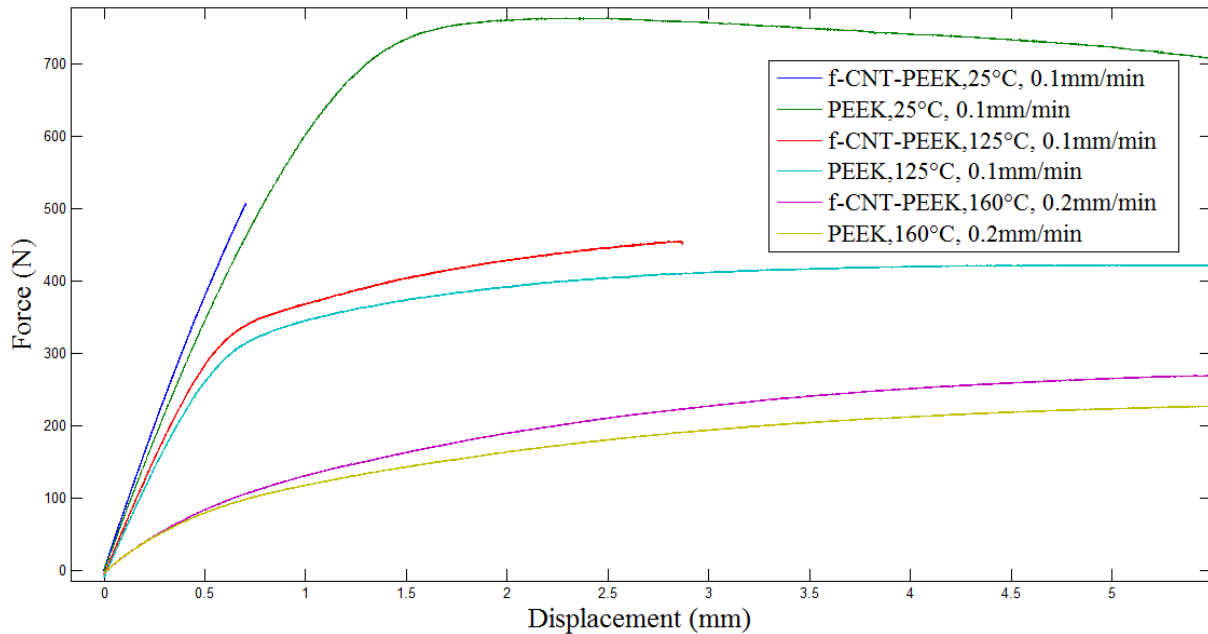


Figure 2. Tensile test for both functionalized CNT-PEEK and neat PEEK.

From Figure 2 it can be observed that both specimens initially display linear behaviour. The CNT reinforced specimen is consistently stiffer than the matrix; however it is also more brittle. This is particularly the case when the matrix is in its glassy regime (in the case of 25°C).

### 4. Dynamic mechanical analysis

The Young's modulus and loss factor for each material was obtained using dynamic mechanical analysis (DMA). In this case, Metravib Viscoanalyser VA1000 system was used. Prismatic shapes were cut from the dog-bone specimens to fit in the tension-compression grips on the test machine. For each measurement, the force required to produce a sinusoidal displacement of given frequency and amplitude was measured. The complex dynamic stiffness of the specimen, and hence the complex Young's modulus, was obtained from this.

#### 4.1 Temperature sweep test

Properties were measured at 1 Hz and dynamic strain amplitude of (0.001mm/mm) while the temperature was ramped at 3 °C/minute. Results are shown in Figures 3 and 4.

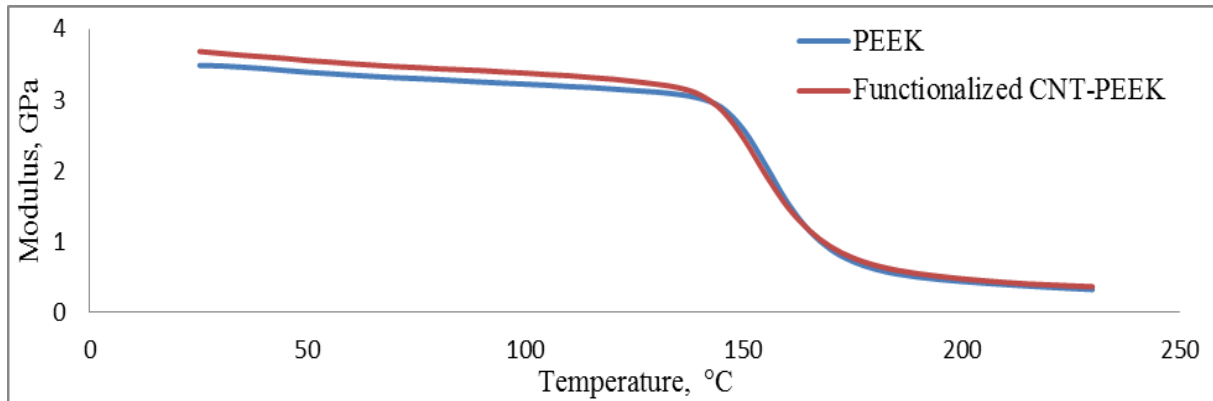


Figure 3. Storage modulus at 1 Hz and dynamic strain (0.001mm/mm)

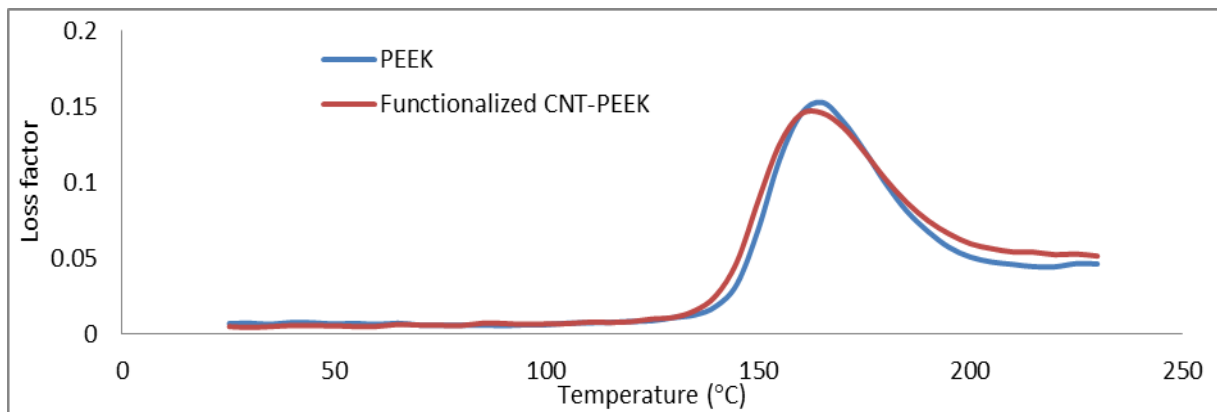


Figure 4. Loss factor at 1 Hz and dynamic strain (0.001mm/mm).

It can be seen that nanotubes tend to increase modulus at lower temperatures. CNTs also produced an increase in damping coefficient above 140 °C. However, the results were not significantly different.

#### 4.2 Strain sweep test

To identify dependence on strain amplitude, a test was carried out at 23°C. Here, the frequency was held at 5 Hz while the dynamic strain amplitude was gradually increased. Results are shown in Figures 5 and 6. It can be seen that as the amplitude increases, Young’s modulus drops and damping rises. These effects are slightly more pronounced for the nanocomposite.

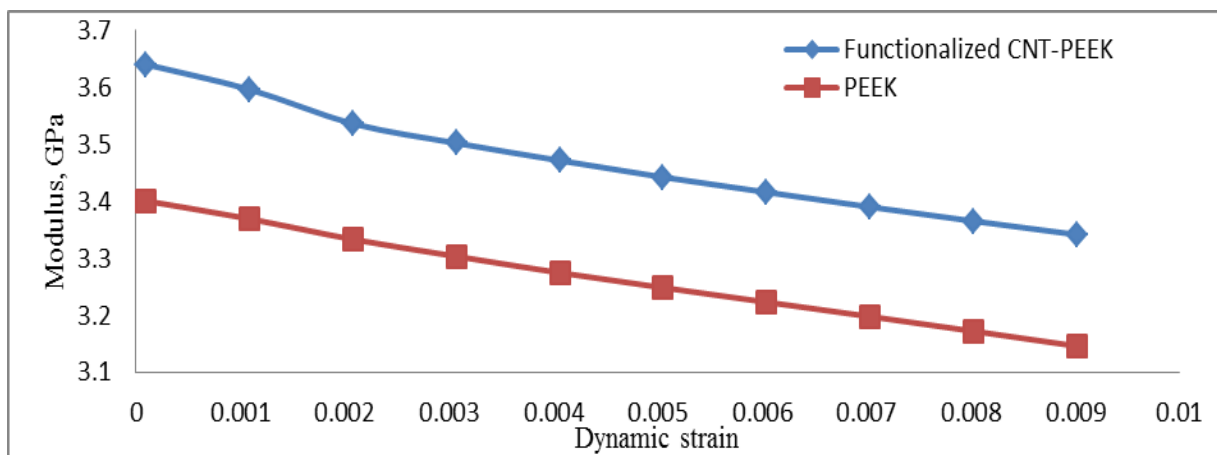


Figure 5. Young’s modulus at 5 Hz and 23°C.

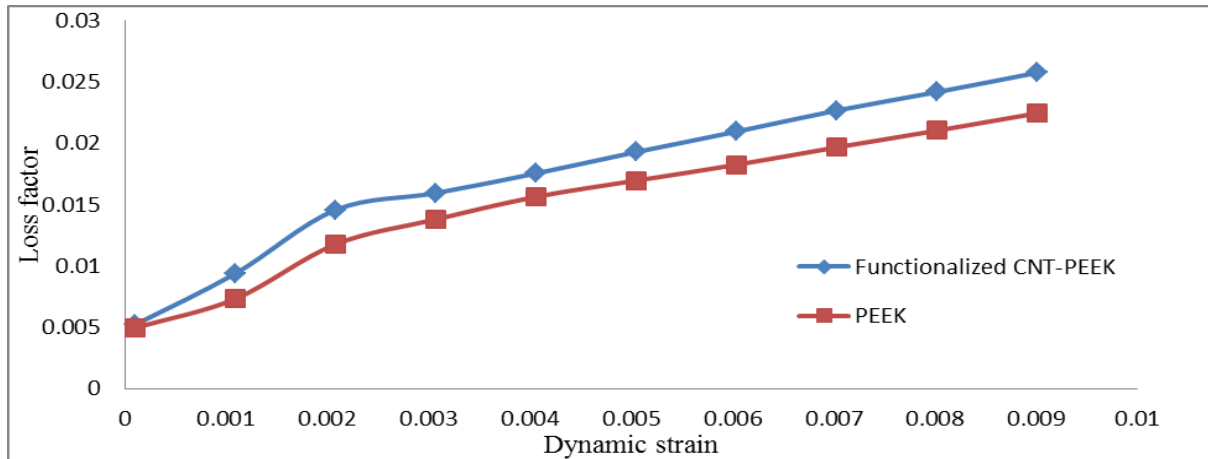


Figure 6. Loss factor at 5 Hz and 23°C

### 3.3 Master curve

Young's modulus and loss factor data were obtained for dynamic strain of  $10^{-3}$ , temperature from 25 to 280 °C in 5°C steps and frequencies from 1 to 31.4 Hz in 7 logarithmic steps. From these, the viscoelastic master curve was constructed. The master curve for PEEK obtained in this way is presented in Figure 7. Measured data points are superimposed as dots. From these curves, properties at any frequencies and temperatures could be obtained.

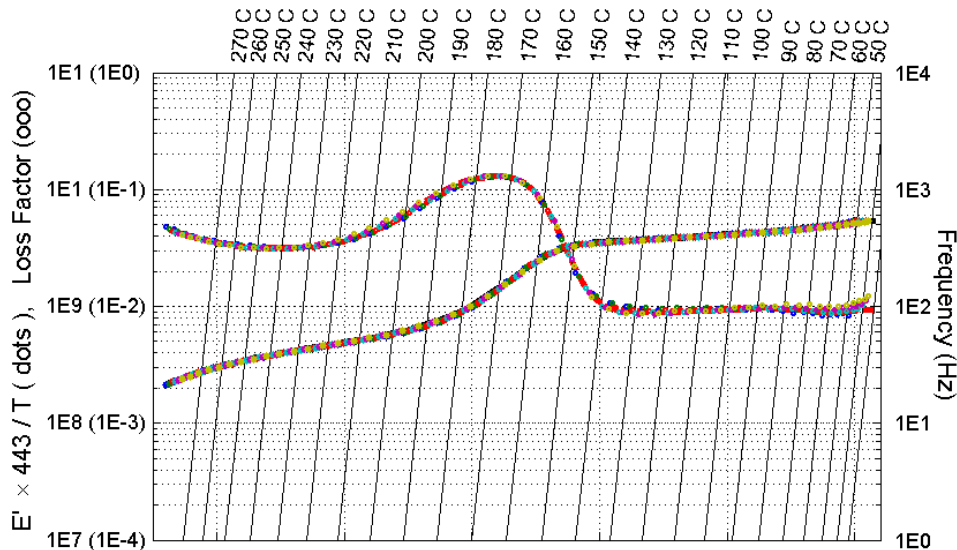


Figure 7. Master curve nomograph for PEEK.

## 5. Numerical model

In this work, a RVE along with the bond-slip numerical method has been used to investigate the interface zone between the fibre and the polymer. In this method, the sliding behaviour is modelled as friction between the fibre and matrix. The volume of interface zone is neglected.

### 5.1 RVE

Properties used in the RVE are given in Table 1. Boundary conditions used are shown in Equations 1, 2 and 3, and Figure 8.

	Material properties			Sizes, $\mu\text{m}$					Volume fraction %
	Young's modulus GPa	Poisson's ratio	density, $\text{kg/m}^3$	length	width	height	inner diameter	outer diameter	
CNT	1000	0.2	1400	0.45	n/a	n/a	0.01	0.02	0.5
PEEK	3.9	0.4	1320	0.5	0.2059	0.2059	n/a	n/a	99.5

**Table 1.** Properties of constituent parts of the nanocomposite.

$$u_1\left(x, \frac{y}{2}, z\right) = 0, u_1\left(x, \frac{-y}{2}, z\right) = 0 \quad (1)$$

$$u_2\left(\frac{x}{2}, y, z\right) = 0, u_2\left(\frac{-x}{2}, y, z\right) = 0 \quad (2)$$

$$u_3\left(x, y, \frac{z}{2}\right) = 0, u_3\left(x, y, \frac{-z}{2}\right) = \Delta L \quad (3)$$

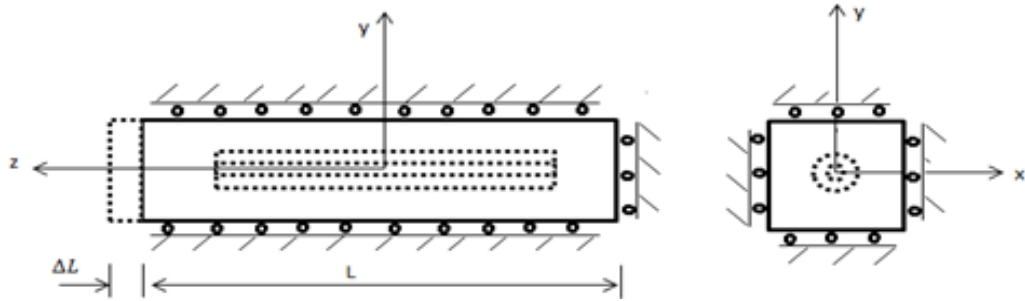


**Figure 8.** Boundary conditions for the RVE model.

### 5.2 Material's behaviour

In the time domain, finite strain behaviour was considered. The model had to represent hyperelasticity and viscoelasticity in addition to the friction slip. A Neo-Hookean (linear) model was used for the hyperelastic behaviour. The viscoelasticity of the matrix was represented using a Prony series (time domain implementation of the Generalized Maxwell model [14]) with parameters obtained by curve fitting in the frequency domain to properties at a particular temperature.

The stress-strain relation for the generalised Maxwell model is given by:

$$\sigma(t) = E_{\infty} \varepsilon(0) + \sum_{i=1}^N E_i e^{-t/\tau_i} \varepsilon(0) \quad (4)$$

where the relaxation modulus is:

$$E(t) = E_{\infty} + \sum_{i=1}^N E_i e^{-t/\tau_i} \quad (5)$$

and the relaxation moduli  $E_i$  and  $\tau_i = \eta_i/E_i$  relaxation time respectively are for the  $i$ -th Maxwell-element. This can be rewritten in relative terms for shear modulus as:

$$\frac{G_R(t)}{G_0} = 1 - \sum_{i=1}^N g_i^{-p} (1 - e^{-t/\tau_i}) \quad (6)$$

$$G_0 = G + \sum_{i=1}^N G_0 g_i^{-p} \quad (7)$$

where ( $N$ ) is the number of terms in the Prony series,  $g_i^{-p}$  is relative modulus of term ( $i$ ),  $\tau_i$  relaxation time of term ( $i$ ) and  $G_0$  is the instantaneous shear modulus.

### 5.3 Numerical bond-slip results

For numerical analysis, the Prony series parameters at temperature 170 °C are listed in Table 2 were used:

No.	g	$\tau$	No.	g	$\tau$
1	0.015208	1.2452e+017	11	0.092147	1.1159e-2
2	0.0072171	1.5505e+015	12	0.16307	1.3895e-4
3	0.0088494	1.9307e+013	13	0.13955	1.7302e-6
4	0.0094729	2.4041e+011	14	0.15617	2.1544e-8
5	0.0077568	2.9936e+009	15	0.042322	2.6827e-1
6	0.011733	3.7276e+007	16	0.025742	3.3405e-12
7	0.012956	4.6416e+005	17	0.026403	4.1596e-14
8	0.018551	5.7797e+003	18	0.02309	5.1795e-16
9	0.037926	7.1969e+001	19	0.029856	6.4495e-18
10	0.050305	8.9615e-1	20	0.049474	8.0309e-2

**Table 2.** Prony series parameters for PEEK at 170 °C.

In order to find the effect of the bond strength between the fibre and the matrix on the nanocomposite mechanical properties, different coefficients of friction were used. Figures 9 and 10 show the effect of friction on the stiffness and loss factor of nanocomposite.

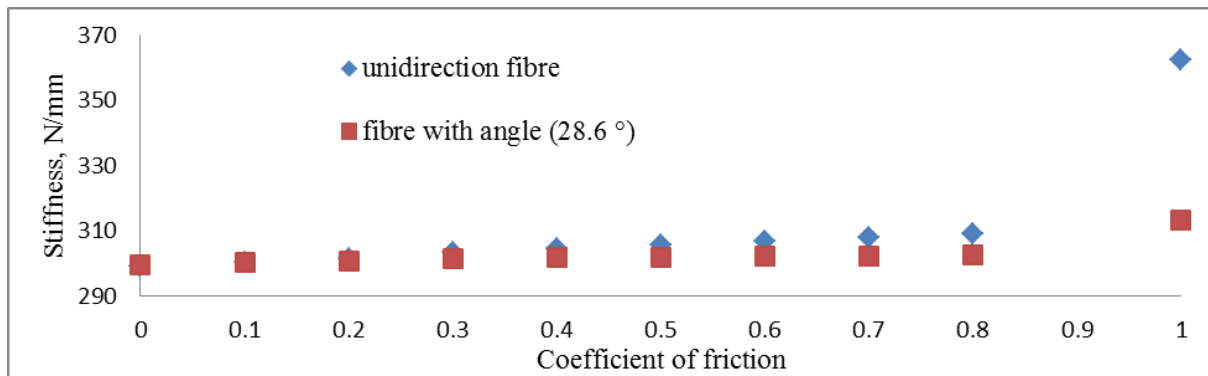


**Figure 9.** Stiffness at different coefficient of friction and fibre end space with viscoelastic matrix.

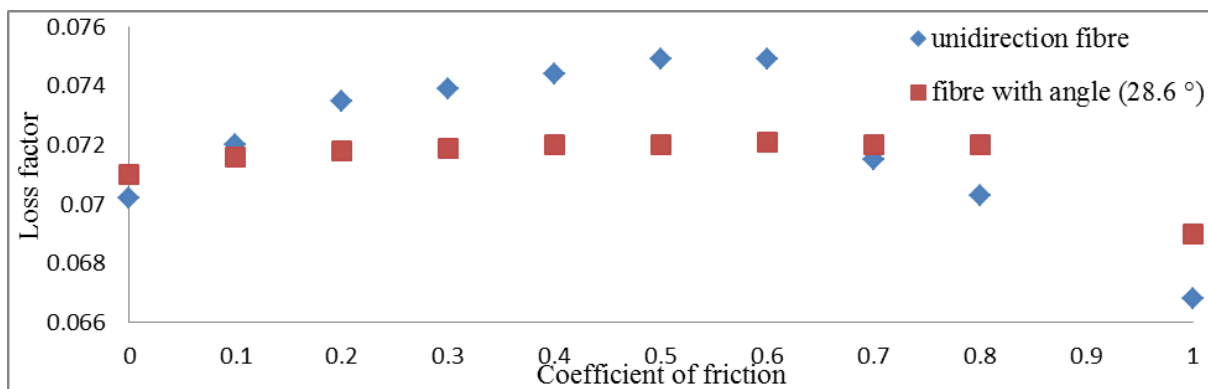


**Figure 10.** Loss factor at different coefficient of friction for both uni-direction fibre and with angle (28.6°).

It can be seen that stiffness increases gradually with friction. Loss factor increases for low coefficient of friction, then declines when the coefficient exceeds 0.5. This appears to be realistic, as with the high bond strength, low degree of slip will occur. It can also be seen that the effect of friction in uni-directional fibre is higher than that of the inclined fibre with an angle of 28.6°.



In this model, it was observed that the hysteresis loop areas in tension and compression are different. Peak stresses on the fibre in compression are nearly ten times higher compared to those in tension. This is caused by the interface model since in tension the interfaces can move apart.

## **6. Conclusions**

Results of experimental and numerical studies on a nanocomposite material (PEEK with functionalised carbon nanotubes) have been presented in this paper. The experimental results showed that the stiffness increased and the ductility was decreased with the addition of nanotubes. Overall strength was only significantly increased at higher temperatures. Sinusoidal testing at different amplitudes showed that damping increased somewhat with the variation in amplitude, while the stiffness decreases. The presence of nanotubes increased this effect only slightly.

A numerical RVE approach was used to investigate the effects of the interface strength on the overall performance. It was shown that nanocomposite stiffness increased with friction gradually. However, the loss factor dropped after coefficient of friction exceeded 0.5.

## **7. Acknowledgments**

This work has been supported by both of the European Community FP7 Collaborative Project ‘‘M-RECT-Multiscale reinforcement of semicrystalline thermoplastic sheets and honeycombs’’ (FP7-NMP-2009-2.5-1), and Kurdistan government (KRG).

## **8. References**

- [1] C. Sun and R. Vaidya. Prediction of composite properties from a representative volume element. *Composite science and technology*, 56: 171-179, 1996.
- [2] S. Reich, C. Thomsen and Maultzsch. *Carbon nanotubes*. Wiley-VCH Verlag, 2004.
- [3] P. Michelis and J. Vlachopoulos, Complete CNT disentanglement dispersion functionalization in a pulsating micro-structured reactor. *Chemical Engineering Science*, 90: 10–16, 2013.
- [4] S. Kurtz. *PEEK biomaterial handbook*. Elsevier Inc. UK, 2012.
- [5] A Díez-Pascual, J. Guan, B. Simard, and M Gómez-Fatou, Polyphenylene sulphide and poly(ether ether ketone) composites reinforced with single-walled carbon nanotube buckypaper.. II- Mechanical properties, electrical and thermal conductivity. *Composites*, 43: 1007–1015, 2012.
- [6] A. Diez-Pascual (and 7 co-authors). High performance PEEK/carbon nanotube composites compatibilized with polysulfones - II mechanical and electrical properties. *Carbon*, 48: 3500–3511, 2010.
- [7] A. Diez-Pascual, (and 6 co-authors). The influence of compatibilizer on the thermal and dynamic mechanical properties of PEEK/carbon nanotube composites. *Nanotechnology*, 20, 2009.
- [8] A. Desai and M. Haque. Mechanics of the interface for carbon nanotubepolymer composites. *Thin-Walled Structures*, 43: 1787–1803, 2005.
- [9] Toshio Ogasawara et. al. Stress–strain behavior of multi-walled carbon nanotube/PEEK composites. *Composites Science and Technology*, 71: 73-78, 2011.
- [10] G. Yogeewaran. Interface toughness of carbon nanotube reinforced epoxy composites. *Applied Material Interface*, 3: 129–134, 2011.
- [11] A. Barber, S. Cohen, H. Wagner, 2003. Measurement of carbon nanotube polymer interfacial strength. *Applied Physics*, 82: 4140–4142, 2003.
- [12] C. DeValve and R. Pitchumani. Experimental Investigation of the Damping Enhancement in Fiber-reinforced Composites with Carbon Nanotubes. *Carbon* 63: 71-83, 2013.
- [13] D. Savvas, V. Papadopoulos and M. Papadrakakis, The effect of interfacial shear strength on damping behavior of carbon nanotube reinforced composites, *International Journal of Solids and Structures*, 49(26), 3823-3937, 2012..
- [14] M. Zmindak et. al. Finite element analysis of viscoelastic composite solids. *Modelling of mechanical and mechatronic systems*, 4, 576-585, 2011.